

ULTRA-CLOSE ENCOUNTERS OF STARS WITH MASSIVE BLACK HOLES:
TIDAL DISRUPTION EVENTS WITH PROMPT HYPERACCRETIONCHRISTOPHER EVANS¹, PABLO LAGUNA¹, AND MICHAEL ERACLEOUS^{2,1}*Draft version August 18, 2021*

ABSTRACT

A bright flare from a galactic nucleus followed at late times by a $t^{-5/3}$ decay in luminosity is often considered the signature of the complete tidal disruption of a star by a massive black hole. The flare and power-law decay are produced when the stream of bound debris returns to the black hole, self-intersects, and eventually forms an accretion disk or torus. In the canonical scenario of a solar-type star disrupted by a $10^6 M_\odot$ black hole, the time between the disruption of the star and the formation of the accretion torus could be years. We present fully general relativistic simulations of a new class of tidal disruption events involving ultra-close encounters of solar-type stars with intermediate mass black holes. In these encounters, a thick disk forms promptly after disruption, on timescales of hours. After a brief initial flare, the accretion rate remains steady and highly super-Eddington for a few days at $\sim 10^2 M_\odot \text{ yr}^{-1}$.

Subject headings: black holes, accretion

1. INTRODUCTION

Observations of tidal disruption events (TDEs) have the potential to unveil super-massive black holes (BHs) at the centers of galaxies. In galaxies with quiescent BHs, accretion-powered nuclear activity is absent, and TDE signatures are, in principle, readily identifiable. The observational evidence for TDEs is rapidly accumulating (Gezari et al. 2012, 2009, 2006; van Velzen et al. 2011; Donato et al. 2014; Levan et al. 2011; Cenko et al. 2012; Chornock et al. 2014; Arcavi et al. 2014; Maksym et al. 2010, 2013). A variety of theoretical scenarios have been considered to explain recent observations, ranging from the traditional case of a disrupted main-sequence star, to more exotic events involving the total or partial disruption of evolved stars such as a white-dwarfs (e.g., Clausen & Eracleous 2011; Krolik & Piran 2011), red-giants (e.g., Davies & King 2005; Bogdanović et al. 2014), horizontal branch stars (e.g., Clausen et al. 2012), and even super-Jupiters (e.g., Nikolaïjuk & Walter 2013). Of particular interest are the theoretical models predicting ignition (e.g., Rosswog et al. 2009) or the amplification of magnetic fields to launch relativistic jets (e.g., Giannios & Metzger 2011; Shcherbakov et al. 2013; Coughlin & Begelman 2014; Tchekhovskoy et al. 2014; Kelley et al. 2014). The motivation behind our work is that, as the number of putative TDE observations grows, more simulations are needed to interpret the wealth of observational data.

TDE modeling was pioneered by Rees (1988), Phinney (1989), and Evans & Kochanek (1989). These studies were first in pointing out that, for the most likely scenario of the disruption of a main-sequence star by a $10^{6-7} M_\odot$ BH, an UV/X-ray flare followed by a $t^{-5/3}$ decay in luminosity should be expected. The flare and

decay are produced by the accretion of bound stellar debris returning to the BH. In particular, the $t^{-5/3}$ decay was singled-out as a ubiquitous signature for the presence of massive BHs. Subsequent studies have incorporated detailed micro-physics (Lodato et al. 2009; Guillochon & Ramirez-Ruiz 2013; Rosswog et al. 2009), considered a wider variety of stellar objects, such as white-dwarfs and red-giants (Shcherbakov et al. 2013; Haas et al. 2012; Kobayashi et al. 2004; Rosswog et al. 2009; Bogdanović et al. 2014), covered longer dynamical times (Guillochon et al. 2009), and included better descriptions of gravity for ultra-close encounters (Laguna et al. 1993; Rosswog 2010; Cheng & Bogdanović 2014).

A challenging aspect of TDE studies is modeling the formation of the accretion disk (Shen & Matzner 2014; Coughlin & Begelman 2014; Cannizzo 1992; Cannizzo et al. 1990). The complication arises because, in canonical TDEs, the time between the disruption of the star and the formation of the accretion disk amounts to several orbital periods of the stellar debris in highly eccentric orbits. This translates into years for a solar-type star disrupted by a $10^6 M_\odot$ BH. For reference, numerical simulations in these cases cover at most a few tens of hours.

Recent papers have addressed the circularization of the returning debris with a variety of methods. Shiohara et al. (2015) found that the debris circularizes at a larger radius than previously thought, and that the accumulation of mass in the ensuing ring is fairly slow. Guillochon & Ramirez-Ruiz (2015) considered the self-intersection of thin post-disruption streams for an ensemble of events and concluded that streams *typically* self-intersect at large distances from the BH, leading to a long viscous time, hence a long delay before the onset of rapid accretion. Bonnerot et al. (2015) and Hayasaki et al. (2015) pointed out the importance of cooling on the rate of circularization of the debris, concluding that efficient cooling leads to very long circularization time scales, hence a delay in the onset of accretion. The picture emerging from the studies is that, although accretion

plaguna@gatech.edu

¹Center for Relativistic Astrophysics and School of Physics
Georgia Institute of Technology, Atlanta, GA 30332²Department of Astronomy & Astrophysics and Institute for
Gravitation and the Cosmos, The Pennsylvania State University,
University Park, PA 16802

could be prompt under the right conditions, it is likely that the onset of accretion is delayed by an appreciable amount of time, perhaps of order a year.

Our study introduces a new class of TDEs, for which a puffed disk or torus forms promptly after disruption. Furthermore, the BH accretes at a steady and highly super-Eddington rate of about $10^2 M_\odot \text{ yr}^{-1}$ for a few days. This highly super-Eddington rate resembles those found by Coughlin & Begelman (2014). Our TDEs involve ultra-close encounters between low mass ($0.57 - 1 M_\odot$) stars and a $10^5 M_\odot$ BH. TDEs with intermediate mass BHs, but larger separation encounters, have been also studied by Ramirez-Ruiz & Rosswog (2009). Our simulations are in a regime where accounting for full general relativistic effects is needed, including those from the spin of the BH. In these ultra-close encounters, the star is effectively disrupted as it arrives at periastris, with the tidal debris plunging into the BH almost instantaneously (on the timescale of one orbital period). Moreover, given the extreme proximity of the debris to the BH, general relativistic precession is very efficient in circularizing stellar material to form an expanding torus. The inner material in the torus spirals into the BH and is accreted at a constant rate until the supply of bound debris is exhausted.

2. TIDAL DISRUPTIONS AT A GLANCE

A star of mass M_* and radius R_* approaching a BH of mass M_h , likely in a highly eccentric or parabolic orbit (Rees 1988; Magorrian & Tremaine 1999; Hayasaki et al. 2012), will be disrupted by tidal forces if it wanders within a distance to the BH

$$R_t \equiv R_* \left(\frac{M_h}{M_*} \right)^{1/3}, \quad (1)$$

called the *tidal radius*. It is customary to characterize the strength of a TDE encounter by its *penetration factor* β , which is defined as

$$\beta \equiv \frac{R_t}{R_p} = \frac{R_*}{R_p} \left(\frac{M_h}{M_*} \right)^{1/3}, \quad (2)$$

with R_p the periastris distance. The fourth length scale in the problem is the gravitational radius $R_g = G M_h / c^2$, which is equal to half the horizon radius for a non-spinning BH and the full horizon radius for a maximally rotating BH.

Given R_* , R_t , R_p and R_g , it is useful to identify the domain of astrophysical relevance of TDEs (Luminet & Pichon 1989). In the β vs M_h plane, this domain is the triangle shown in Figure 1, whose demarcations are obtained by interpreting β in Eq. (2) as a function of R_p . The base of the triangle is $R_p = R_t$, i.e. $\beta_t \equiv \beta(R_t) = 1$. Below this line ($R_p > R_t$) there is no disruption. The left side of the triangle is the line obtained by setting $R_p = R_*$; that is,

$$\beta_* \equiv \beta(R_*) = \left(\frac{M_h}{M_*} \right)^{1/3}. \quad (3)$$

To the left of this line ($R_p < R_*$) lie very close encounters where *the BH enters the star* in the process of disrupting it. This process has many similarities to the high-speed collisions of stellar-mass BHs and red giants as studied by

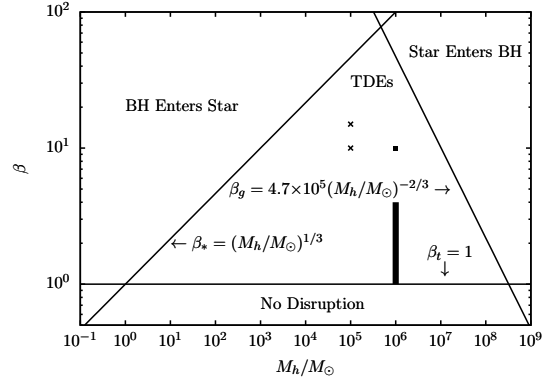


FIG. 1.— Tidal disruption domain for a $M_* = M_\odot$ BH and $R_* = R_\odot$ star. The thick vertical line denotes canonical TDEs. The square point shows the ultra-close TDE from Laguna et al. (1993) and crosses those in the present study.

Dale et al. (2009). Finally, the right side of the triangle is the line when $R_p = R_g$; that is,

$$\beta_g \equiv \beta(R_g) = \frac{R_*}{G M_h / c^2} \left(\frac{M_h}{M_*} \right)^{-2/3}. \quad (4)$$

To the right of this line ($R_p < R_g$) are events where the *star enters the BH* before it is disrupted.

According to Figure 1, for a solar-type star ($M_* = M_\odot$ and $R_* = R_\odot$), the maximum BH mass to disrupt the star is $M_h = 3.2 \times 10^5 M_\odot$. Moreover, the maximum penetration factor with disruption is $\beta = 78$, which involves a $M_h = 4.7 \times 10^5 M_\odot$ BH. The edges of the triangle of astrophysical relevance are, of course, not sharp due to variations in the definition of relevant length scales arising from the spin of the BH, the space-time curvature in the neighborhood of the BH, and the internal structure of the star.

After disruption, the receding debris spreads, with roughly half of the material remaining bound to the BH. The most bound material has specific binding energy given by

$$e_{\min} \simeq - \frac{G M_h \Delta R_*}{R_f^2} \simeq -G \beta^2 f^{-2} \xi M_*^{2/3} R_*^{-1} M_h^{1/3}, \quad (5)$$

where $\Delta R_* = \xi R_*$ is the spread of the debris with ξ a deformation factor, and

$$R_f = \frac{R_t}{\beta} [\beta n + (1 - n)] = \frac{R_t}{\beta} f(\beta, n) \quad (6)$$

is the distance to the hole when the spread in specific binding energy of the debris freezes-in. In the original estimates (Evans & Kochanek 1989), $n = 0$ ($f = 1$), and thus $R_f = R_p$. More recent studies (Stone et al. 2013; Guillochon & Ramirez-Ruiz 2013) suggest that $n = 1$ ($f = \beta$), so $R_f = R_t$. In our study, we observed that $n \sim 0.5$, which for large β translates to $f \sim 0.5$.

With e_{\min} at hand, the characteristic fallback time for

the most tightly bound material to return to the BH is

$$t_{\min} \simeq 2\pi \frac{G M_h}{(2|e_{\min}|)^{3/2}} \simeq \frac{\pi}{\sqrt{2G}} \beta^{-3} f^3 \xi^{-3/2} R_*^{3/2} M_*^{-1} M_h^{1/2}. \quad (7)$$

Furthermore, from the Keplerian relation

$$\frac{de}{dt} = \frac{1}{3} (2\pi G M_h)^{2/3} t^{-5/3} \quad (8)$$

and the mass per specific binding energy

$$\frac{dM_h}{de} \simeq \frac{M_*}{2|e_{\min}|} \simeq \frac{M_*}{t_{\min}^{-2/3}} \frac{1}{(2\pi G M_h)^{2/3}}, \quad (9)$$

which is assumed to be roughly constant, the accretion rate is estimated to be

$$\dot{M}_h \equiv \frac{dM_h}{dt} = \frac{dM_h}{de} \frac{de}{dt} \simeq \dot{M}_{\max} \left(\frac{t}{t_{\min}} \right)^{-5/3}, \quad (10)$$

with $\dot{M}_{\max} \equiv M_*/(3t_{\min})$. The power-law decay of $t^{-5/3}$ in Eq. (10) is considered to be a ubiquitous property of TDEs (Rees 1988; Evans & Kochanek 1989; Laguna et al. 1993; Rosswog et al. 2009). Slight departures from this power-law have been found close to the peak accretion rate as a result of the equation of state of the star (Lodato et al. 2009) or effects from the spin of the massive BH (Haas et al. 2012). Recent work by Guillochon & Ramirez-Ruiz (2013) has shown that the canonical $t^{-5/3}$ characterizes only full tidal disruptions.

In the case of a TDE with $M_* = M_\odot$, $R_* = R_\odot$ and $M_h = 10^6 M_\odot$,

$$t_{\min} \simeq 0.11 \beta^{-3} f^3 \xi^{-3/2} r_*^{3/2} m_*^{-1} M_6^{1/2} \text{ yr}, \quad (11)$$

and

$$\dot{M}_{\max} \simeq 0.3 \beta^3 f^{-3} \xi^{3/2} r_*^{-3/2} m_*^2 M_6^{-1/2} M_\odot \text{ yr}^{-1}, \quad (12)$$

where $M_6 \equiv M_h/10^6 M_\odot$, $r_* \equiv R_*/R_\odot$ and $m_* \equiv M_*/M_\odot$. For comparison, the Eddington accretion rate in this situation is $\dot{M}_{\text{Edd}} = 0.02 M_6 M_\odot \text{ yr}^{-1}$ (assuming 10% efficiency).

3. NEW TDE REGIME

We are interested in TDEs with $\beta = 10$ and 15, involving a BH with mass $M_h = 10^5 M_\odot$. They are denoted by crosses in Figure 1 and are closer to the *BH-enters-star* boundary than the “canonical” scenarios of $\beta = \text{few}$ and $M_h = 10^6 M_\odot$, which are denoted by a thick vertical line in Figure 1. In the same figure, the square point shows the ultra-close TDE from Laguna et al. (1993). Here, we consider non-spinning BHs and BHs with spin $a/M_h = \pm 0.65$. The sign denotes whether the spin of the BH is aligned (plus) or anti-aligned (minus) with the orbital angular momentum of the star. The disruptions involve main-sequence stars injected in parabolic orbits with masses $M_* = 1 M_\odot$ and $0.57 M_\odot$, modeled as polytropes with equation of state $p \propto \rho_0^\Gamma$ and $\Gamma = 4/3$. During the evolution, we use a gamma-law equation of state $p = \rho_0 \epsilon (\Gamma - 1)$. Table 1 provides the parameters of the simulations: the penetration factor β , the BH spin parameter a , and the mass of the star M_* .

The simulations were carried out with our Maya code and fully account for general relativistic effects. This code was also used in our previous general relativistic TDE study (Haas et al. 2012). The Maya code is 4th order accurate in solving the Einstein equations and 2nd order in the hydrodynamics equations. The general convergence of the code is slightly above 2nd order. We employ nine levels of mesh refinements. All but the coarsest mesh have 70^3 grid-points, with the coarsest having 120^3 . The resolution on the finest mesh is $R_g/50$.

In general terms, the TDEs studied here involve stars comparable in size to the BH, $R_* \simeq 4.7 M_5^{-1} r_* R_g$, periastron distances of about

$$R_p \simeq 4.64 \beta_{10}^{-1} M_5^{1/3} m_*^{-1/3} R_*, \quad (13)$$

and tidal radius

$$R_t \simeq 218 M_5^{-2/3} m_*^{-1/3} r_* R_g, \quad (14)$$

where $M_5 \equiv M_h/10^5 M_\odot$ and $\beta_{10} \equiv \beta/10$. Although the value of R_p suggests that the star could potentially swing by the BH without the BH entering the star, the combination of large β and general relativistic effects produce an outcome dramatically different from the situations with $\beta \sim 1$ and $10^6 M_\odot$ mass BHs (next section).

With $\beta \geq 10$ and intermediate mass BHs, the star will be effectively disrupted and stretched to a few times its original size by the time it reaches periastron passage. A deformation factor $\xi \simeq 4$ was found to be common in our simulations. Therefore, from Eqs. (7) and (10)

$$t_{\min} \simeq 137 \beta_{10}^{-3} f^3 \xi_4^{-3/2} r_*^{3/2} m_*^{-1} M_5^{1/2} \text{ s}, \quad (15)$$

and

$$\dot{M}_{\max} \simeq 9.6 \times 10^3 \beta_{10}^3 f^{-3} \xi_4^{3/2} r_*^{-3/2} m_*^2 M_5^{-1/2} M_\odot \text{ yr}^{-1}, \quad (16)$$

where $\xi_4 = \xi/4$. For reference, the Eddington accretion rate in this case is $\dot{M}_{\text{Edd}} = 0.002 M_5 M_\odot \text{ yr}^{-1}$. Our simulations show that $\dot{M}_{\max} \sim 10^4 M_\odot \text{ yr}^{-1}$ and $t_{\min} \sim 25 \text{ s}$. This time-scale is comparable to the circular orbital period of the most bound material:

$$\begin{aligned} P_{\text{circ}} &= 2\pi \sqrt{\frac{(R_p - \Delta R_*)^3}{G M_h}} \\ &\simeq 316 (1 - \Delta R_*/R_p)^{3/2} \beta_{10}^{-3/2} r_*^{3/2} m_*^{-1/2} \text{ s} \\ &\simeq 16.5 \beta_{10}^{-3/2} r_*^{3/2} m_*^{-1/2} \text{ s}, \end{aligned} \quad (17)$$

where $\Delta R_*/R_p \simeq 0.86 \xi_4 \beta_{10}^{1/3} M_5^{1/3}$.

4. ANATOMY OF A DISRUPTION

We focus this discussion chiefly on the accretion rates onto the BH. Figure 2 shows the accretion rates of tidal debris through the BH horizon. The time axis is such that $t = 0 \text{ s}$ denotes periastron passage. Three distinct accretion epochs or stages are identifiable in most of the cases.

The first phase is a narrow spike or flare in the accretion rate. The spike is due to the portion of the stellar debris that immediately plunges into the BH. An esti-

TABLE 1
SIMULATION PARAMETERS AND ACCRETION RATES.

Run	β	a/M_h	M_*/M_\odot	$\dot{M}_{\max} (M_\odot \text{ yr}^{-1})$	$\dot{M}_{\text{late}} (M_\odot \text{ yr}^{-1})$
$\beta_{10} S_0 M_1$	10	0	1	3.6×10^2	1.0×10^3
$\beta_{10} S_{0.65} M_1$	10	0.65	1	1.0×10^4	7.5×10^2
$\beta_{10} S_{-0.65} M_1$	10	-0.65	1	1.2×10^5	2.0×10^2
$\beta_{10} S_0 M_{0.57}$	10	0	0.57	3.5×10^2	1.0×10^2
$\beta_{10} S_{0.65} M_{0.57}$	10	0.65	0.57	7.6×10^3	4.0×10^2
$\beta_{10} S_{-0.65} M_{0.57}$	10	-0.65	0.57	7.9×10^4	3.0×10^2
$\beta_{15} S_0 M_{0.57}$	15	0	0.57	2.0×10^4	4.0×10^2
$\beta_{15} S_{0.65} M_{0.57}$	15	0.65	0.57	8.8×10^4	3.5×10^2
$\beta_{15} S_{-0.65} M_{0.57}$	15	-0.65	0.57	3.8×10^5	2.0×10^2

mate of this accretion rate is given by

$$\dot{M}_h \sim A_h \rho_\infty v_\infty \sim 10^4 \beta_{10}^{1/2} M_5^{7/3} m_*^{7/6} r_*^{-7/2} M_\odot \text{ yr}^{-1}, \quad (18)$$

where we have used $A_h \sim 4\pi R_g^2$, $v_\infty \sim (GM_h/R_p)^{1/2}$ and $\rho_\infty \sim M_*/(4\pi R_*^3/3)$. This estimate is consistent with the values for \dot{M}_{\max} reported in Table 1.

After the accretion flare there is a decay phase, which for a non-spinning BH (see top panel in Figure 2) loosely resembles a power-law decay. The duration of this decay seems to depend on the spin of the BH and the penetration factor β .

Finally, as new material returns to the BH, it circularizes and forms an accretion torus on a timescale of $\sim 10 t_{\min} \sim 1,400$ s (Evans & Kochanek 1989), with the accretion eventually reaching steady state at about $\dot{M}_{\text{late}} \sim 10^2 M_\odot \text{ yr}^{-1}$, as noted in the last column of Table 1. The steady state accretion will cease when the mass supply from the bound debris is depleted.

5. SIMULATION RESULTS

To illustrate the effect of the mass of the star, panels A, B and C in Figure 2 show the BH accretion rate for $\beta = 10$, grouping the cases with the same BH spin parameter. Since the accretion rate seems to be insensitive to the mass of the star, we will focus on the $M_* = 0.57 M_\odot$ star given that we have a wider variety of simulations for this star.

In Figure 2, we also organize the runs according to β , with $\beta = 10$ in panel D, and $\beta = 15$ in panel E. The peak accretion rate of the flare is higher if the BH is spinning. Interestingly, the case with a counter-rotating orbit (i.e. BH spin anti-aligned with the orbital angular momentum) yields the largest peak accretion rate. For the $\beta = 10$ simulations, the post-flare accretion rate depends on the BH spin magnitude but not its orientation, which is consistent with similar findings for the steady-state, subsonic accretion onto a moving BH (Petrich et al. 1988). The late-time accretion rate seems to increase with the spin of the BH. Another difference between the $a/M_h = 0$ and the $a/M_h = \pm 0.65$ cases is that for the latter, the time scale for flare decay is shorter; that is, the late constant accretion phase, which signals the formation of the torus, is reached after a couple of hundred seconds.

The corresponding $\beta = 15$ cases show that the spin of the BH does not play a role in determining the late-time, constant accretion rate. Furthermore, as with the $\beta = 10$ cases with spinning BHs, the constant accretion

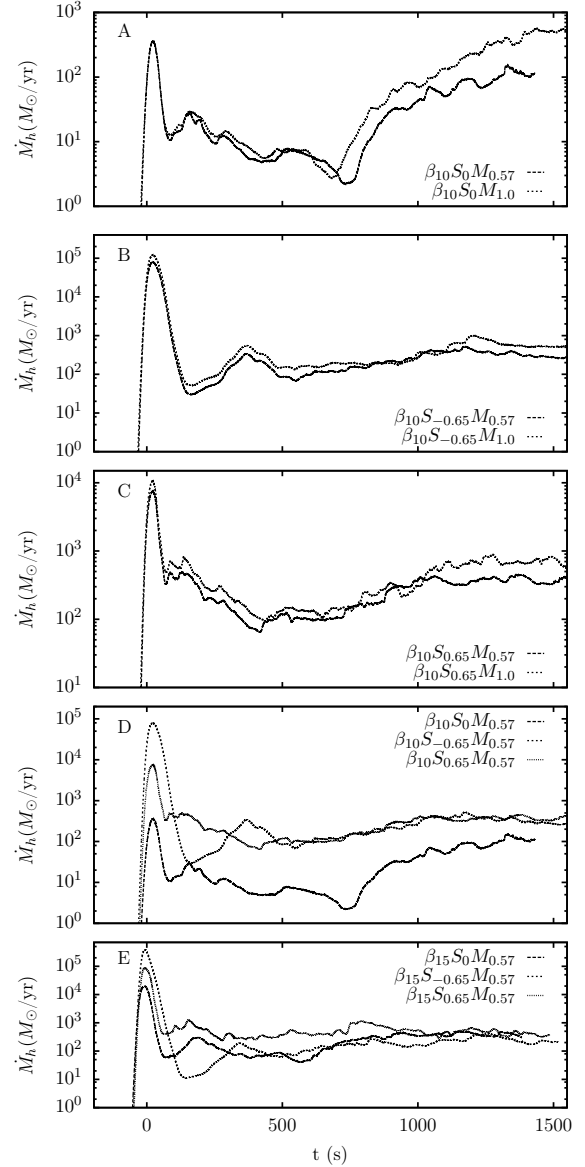


FIG. 2.— BH accretion rate as a function of time. Panels A–C display cases with penetration factor $\beta = 10$ grouped by the spin parameter of the BH, with $a/M_h = 0, -0.65$ and 0.65 corresponding to panels A, B and C, respectively. The remaining panels display accretion rates for $M_* = 0.57 M_\odot$ with penetration factor $\beta = 10$ (panel D) and $\beta = 15$ (panel E).

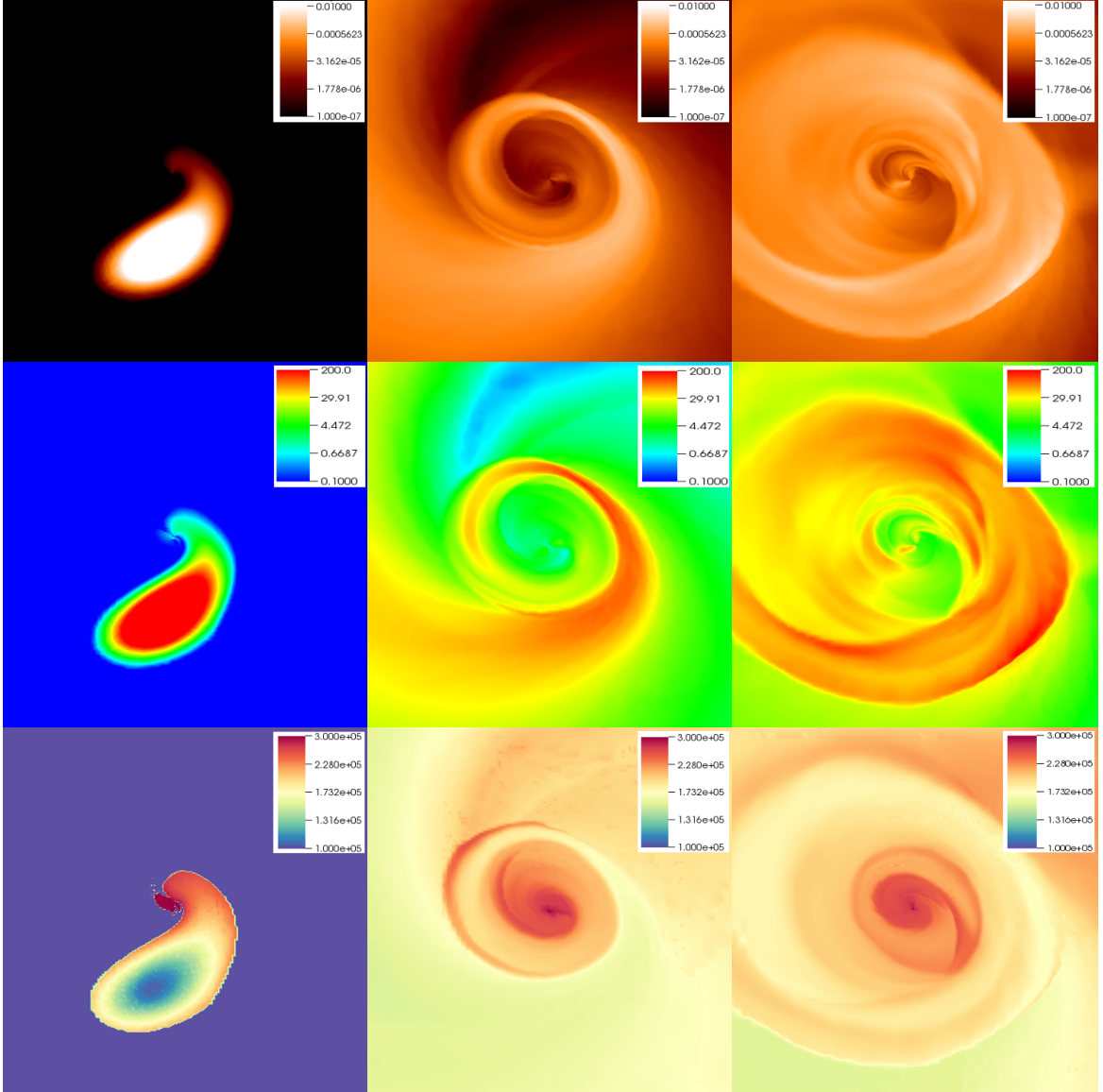


FIG. 3.— Snapshots of the density (top row), temperature (middle row) and specific entropy (bottom row) of the stellar debris for the $\beta_{10}S_0M_{0.57}$ case. Columns from left to right depict times $t = -28$ s, 450 s and 1,250 s, respectively.

phase is reached within a few hundred seconds. For both the $\beta = 10$ and $\beta = 15$ cases, the late-time accretion rate is $\sim 10^2 M_\odot \text{yr}^{-1}$.

In summary, we found that the accretion rate is not very sensitive to M_* , and that the rate reached during the flare depends on both a/M_h and β . Furthermore, the late accretion rate for $\beta = 15$ is not sensitive to the spin of the BH, and for both penetration factors is approximately $\dot{M} \sim 10^2 M_\odot \text{yr}^{-1}$. With the exception of the cases with $\beta = 10$ and $a/M_h = 0, 0.65$ (panels A and C in Figure 2), there are no hints of a power-law decay rate.

Figure 3 shows snapshots of the density (top row), temperature (middle row) and specific entropy (bottom row) of the stellar debris for the $\beta_{10}S_0M_{0.57}$ case. Columns from left to right depict times $t = -28$ s, 450 s and 1,250 s, respectively. Self-intersection of debris and subsequent formation of the accretion torus are evident. The increase in temperature and entropy as a result of shocks due to self-intersection of material is also evident.

Finally, Figure 4 shows histograms of the mass per unit binding energy as a function of binding energy for the same case and times as in Figure 3. It is evident that $dM_h/d\epsilon$ is not flat, as is required to achieve the $t^{-5/3}$ power-law decay.

Carter & Luminet (1982) were first to suggest a tidal compression perpendicular to the orbital plane $\propto \beta^{-3}$ that would yield an increase in the central density and temperature of the star $\propto \beta^3$ and β^2 , respectively. We do not observe such extreme compression. As mentioned before, the star arrives at periastris effectively disrupted, with its central density decaying and undergoing only a mild compression, adequately handled with the resolution used in our simulations.

6. CONCLUSIONS

We presented a new class of TDEs showing prompt formation of an accretion torus and hyperaccretion. These TDEs involve ultra-close encounters with a $M_h = 10^5 M_\odot$ BH. The accretion rates are highly super-

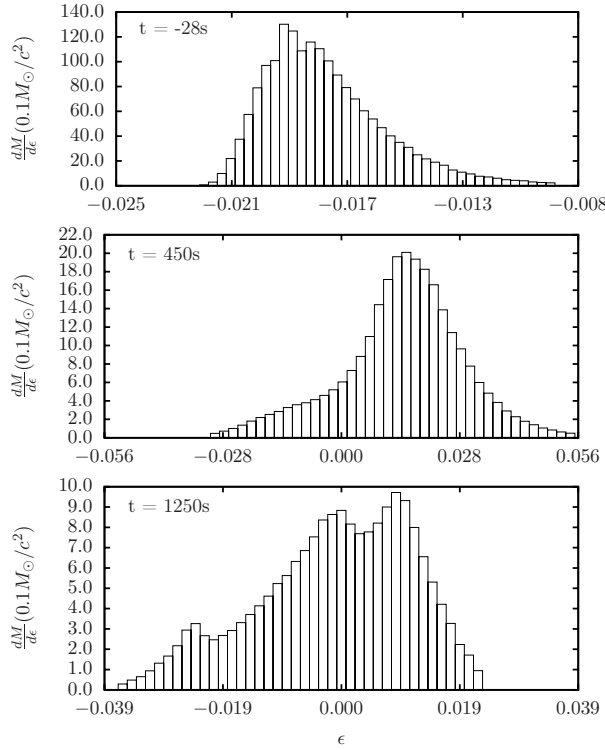


FIG. 4.— Histograms of the mass per unit binding energy as a function of binding energy for the case in Figure 3.

Eddington. Additionally, there is no evidence of a $t^{-5/3}$ decay in the accretion rate. This is likely due the strong influence of general relativistic effects in these ultra-close encounters. The late-time accretion rate, once the torus has formed, reaches an approximate steady-state and remains highly super-Eddington at $\dot{M}_{\text{late}} \sim 10^2 M_{\odot} \text{ yr}^{-1}$. With this rate, the BH should be able to accrete the majority of the bound tidal debris in just a few days. A word of caution is needed regarding the accretion rate quotes in this study. Our simulations did not include effects from radiation, which could potentially decrease the rates. However, it is not likely that radiation effects would diminish the rates enough to make them sub-Eddington, since the Eddington rate in these situations is $\dot{M}_{\text{Edd}} = 0.002 M_5 M_{\odot} \text{ yr}^{-1}$ (assuming 10% efficiency).

In a subsequent study, we will expand the parameter space of our simulations and investigate the emission properties of the tidal debris. It will be important to investigate further the role of shocks in heating and circularizing the debris as well as the overall role of cooling effects. Moreover, we will consider inclined orbits relative to the spin axis of the BH in order to compare our results with those of Shen & Matzner (2014). We are also interested in the possibility of amplification of magnetic fields and whether the class of TDEs in the present study could provide an explanation for jetted events, such as Swift J1644+57 (Burrows et al. 2011; Levan et al. 2011).

We thank Tamara Bogdanović. Work supported by NSF 1205864, 1212433, 1333360. Computations at XSEDE TG-PHY120016.

REFERENCES

- Arcavi, I., Gal-Yam, A., Sullivan, M., Pan, Y.-C., Cenko, S. B., Horesh, A., Ofek, E. O., De Cia, A., Yan, L., Yang, C.-W., Howell, D. A., Tal, D., Kulkarni, S. R., Tendulkar, S. P., Tang, S., Xu, D., Sternberg, A., Cohen, J. G., Bloom, J. S., Nugent, P. E., Kasliwal, M. M., Perley, D. A., Quimby, R. M., Miller, A. A., Theissen, C. A., & Laher, R. R. 2014, *ApJ*, 793, 38
- Bogdanović, T., Cheng, R. M., & Amaro-Seoane, P. 2014, *ApJ*, 788, 99
- Bonnerot, C., Rossi, E. M., Lodato, G., & Price, D. J. 2015, *ArXiv e-prints*
- Burrows, D. N., Kennea, J. A., Ghisellini, G., Mangano, V., Zhang, B., Page, K. L., Eracleous, M., Romano, P., Sakamoto, T., Falcone, A. D., Osborne, J. P., Campana, S., Beardmore, A. P., Breeveld, A. A., Chester, M. M., Corbet, R., Covino, S., Cummings, J. R., D’Avanzo, P., D’Elia, V., Esposito, P., Evans, P. A., Fugazza, D., Gelbord, J. M., Hiroi, K., Holland, S. T., Huang, K. Y., Im, M., Israel, G., Jeon, Y., Jeon, Y.-B., Jun, H. D., Kawai, N., Kim, J. H., Krimm, H. A., Marshall, F. E., P. Mészáros, Negoro, H., Omodei, N., Park, W.-K., Perkins, J. S., Sugizaki, M., Sung, H.-I., Tagliaferri, G., Troja, E., Ueda, Y., Urata, Y., Usui, R., Antonelli, L. A., Barthelmy, S. D., Cusumano, G., Giommi, P., Melandri, A., Perri, M., Racusin, J. L., Sbarufatti, B., Siegel, M. H., & Gehrels, N. 2011, *Nature*, 476, 421
- Cannizzo, J. K. 1992, *ApJ*, 385, 94
- Cannizzo, J. K., Lee, H. M., & Goodman, J. 1990, *ApJ*, 351, 38
- Carter, B. & Luminet, J. P. 1982, *Nature*, 296, 211
- Cenko, S. B., Krimm, H. A., Horesh, A., Rau, A., Frail, D. A., Kennea, J. A., Levan, A. J., Holland, S. T., Butler, N. R., Quimby, R. M., Bloom, J. S., Filippenko, A. V., Gal-Yam, A., Greiner, J., Kulkarni, S. R., Ofek, E. O., Olivares E., F., Schady, P., Silverman, J. M., Tanvir, N. R., & Xu, D. 2012, *Astrophysical Journal*, 753, 77
- Cheng, R. M. & Bogdanović, T. 2014, *Phys. Rev. D*, 90, 064020
- Chornock, R., Berger, E., Gezari, S., Zauderer, B. A., Rest, A., Chomiuk, L., Kamble, A., Soderberg, A. M., Czekala, I., Dittmann, J., Drout, M., Foley, R. J., Fong, W., Huber, M. E., Kirshner, R. P., Lawrence, A., Lunnan, R., Marion, G. H., Narayan, G., Riess, A. G., Roth, K. C., Sanders, N. E., Scolnic, D., Smartt, S. J., Smith, K., Stubbs, C. W., Tonry, J. L., Burgett, W. S., Chambers, K. C., Flewelling, H., Hodapp, K. W., Kaiser, N., Magnier, E. A., Martin, D. C., Neill, J. D., Price, P. A., & Wainscoat, R. 2014, *ApJ*, 780, 44
- Clausen, D. & Eracleous, M. 2011, *ApJ*, 726, 34
- Clausen, D., Sigurdsson, S., Eracleous, M., & Irwin, J. A. 2012, *MNRAS*, 424, 1268
- Coughlin, E. R. & Begelman, M. C. 2014, *ApJ*, 781, 82
- Dale, J. E., Davies, M. B., Church, R. P., & Freitag, M. 2009, *MNRAS*, 393, 1016
- Davies, M. B. & King, A. 2005, *ApJ*, 624, L25
- Donato, D., Cenko, S. B., Covino, S., Troja, E., Pursimo, T., Cheung, C. C., Fox, O., Kutyrev, A., Campana, S., Fugazza, D., Landt, H., & Butler, N. R. 2014, *ApJ*, 781, 59
- Evans, C. R. & Kochanek, C. S. 1989, *Astrophysical Journal Letters*, 346, L13
- Gezari, S., Chornock, R., Rest, A., Huber, M. E., Forster, K., Berger, E., Challis, P. J., Neill, J. D., Martin, D. C., Heckman, T., Lawrence, A., Norman, C., Narayan, G., Foley, R. J., Marion, G. H., Scolnic, D., Chomiuk, L., Soderberg, A., Smith, K., Kirshner, R. P., Riess, A. G., Smartt, S. J., Stubbs, C. W., Tonry, J. L., Wood-Vasey, W. M., Burgett, W. S., Chambers, K. C., Grav, T., Heasley, J. N., Kaiser, N., Kudritzki, R.-P., Magnier, E. A., Morgan, J. S., & Price, P. A. 2012, *Nature*, 485, 217
- Gezari, S., Heckman, T., Cenko, S. B., Eracleous, M., Forster, K., Gonçalves, T. S., Martin, D. C., Morrissey, P., Neff, S. G., Seibert, M., Schiminovich, D., & Wyder, T. K. 2009, *ApJ*, 698, 1367

- Gezari, S., Martin, D. C., Milliard, B., Basa, S., Halpern, J. P., Forster, K., Friedman, P. G., Morrissey, P., Neff, S. G., Schiminovich, D., Seibert, M., Small, T., & Wyder, T. K. 2006, *ApJ*, 653, L25
- Giannios, D. & Metzger, B. D. 2011, *MNRAS*, 416, 2102
- Guillochon, J. & Ramirez-Ruiz, E. 2013, *ApJ*, 767, 25
- . 2015, *ArXiv e-prints*
- Guillochon, J., Ramirez-Ruiz, E., Rosswog, S., & Kasen, D. 2009, *ApJ*, 705, 844
- Haas, R., Shcherbakov, R. V., Bode, T., & Laguna, P. 2012, *ApJ*, 749, 117
- Hayasaki, K., Stone, N., & Loeb, A. 2012, in *European Physical Journal Web of Conferences*, Vol. 39, *European Physical Journal Web of Conferences*, 1004
- Hayasaki, K., Stone, N. C., & Loeb, A. 2015, *ArXiv e-prints*
- Kelley, L. Z., Tchekhovskoy, A., & Narayan, R. 2014, *MNRAS*, 445, 3919
- Kobayashi, S., Laguna, P., Phinney, E. S., & Mészáros, P. 2004, *ApJ*, 615, 855
- Krolik, J. H. & Piran, T. 2011, *ApJ*, 743, 134
- Laguna, P., Miller, W. A., Zurek, W. H., & Davies, M. B. 1993, *ApJ*, 410, L83
- Levan, A. J., Tanvir, N. R., Cenko, S. B., Perley, D. A., Wiersema, K., Bloom, J. S., Fruchter, A. S., Postigo, A. d. U., O'Brien, P. T., Butler, N., van der Horst, A. J., Leloudas, G., Morgan, A. N., Misra, K., Bower, G. C., Farihi, J., Tunnicliffe, R. L., Modjaz, M., Silverman, J. M., Hjorth, J., Thöne, C., Cucchiara, A., Cerón, J. M. C., Castro-Tirado, A. J., Arnold, J. A., Bremer, M., Brodie, J. P., Carroll, T., Cooper, M. C., Curran, P. A., Cutri, R. M., Ehle, J., Forbes, D., Fynbo, J., Gorosabel, J., Graham, J., Hoffman, D. I., Guziy, S., Jakobsson, P., Kamble, A., Kerr, T., Kasliwal, M. M., Kouveliotou, C., Kocevski, D., Law, N. M., Nugent, P. E., Ofek, E. O., Poznanski, D., Quimby, R. M., Rol, E., Romanowsky, A. J., Sánchez-Ramírez, R., Schulze, S., Singh, N., van Spaandonk, L., Starling, R. L. C., Strom, R. G., Tello, J. C., Vaduvescu, O., Wheatley, P. J., Wijers, R. A. M. J., Winters, J. M., & Xu, D. 2011, *Science*, 333, 199
- Lodato, G., King, A. R., & Pringle, J. E. 2009, *Monthly Notices of the Royal Astronomical Society*, 392, 332
- Luminet, J.-P. & Pichon, B. 1989, *A&A*, 209, 103
- Magorrian, J. & Tremaine, S. 1999, *MNRAS*, 309, 447
- Maksym, W. P., Ulmer, M. P., & Eracleous, M. 2010, *ApJ*, 722, 1035
- Maksym, W. P., Ulmer, M. P., Eracleous, M. C., Guennou, L., & Ho, L. C. 2013, *MNRAS*, 435, 1904
- Nikolajuk, M. & Walter, R. 2013, *A&A*, 552, A75
- Petrich, L. I., Shapiro, S. L., & Teukolsky, S. A. 1988, *Phys. Rev. Lett.*, 60, 1781
- Phinney, E. S. 1989, in *IAU Symposium*, Vol. 136, *The Center of the Galaxy*, ed. M. Morris, 543
- Ramirez-Ruiz, E. & Rosswog, S. 2009, *ApJ*, 697, L77
- Rees, M. J. 1988, *Nature*, 333, 523
- Rosswog, S. 2010, *Classical and Quantum Gravity*, 27, 114108
- Rosswog, S., Ramirez-Ruiz, E., & Hix, W. R. 2009, *ApJ*, 695, 404
- Shcherbakov, R. V., Pe'er, A., Reynolds, C. S., Haas, R., Bode, T., & Laguna, P. 2013, *ApJ*, 769, 85
- Shen, R.-F. & Matzner, C. D. 2014, *ApJ*, 784, 87
- Shiokawa, H., Krolik, J. H., Cheng, R. M., Piran, T., & Noble, S. C. 2015, *ArXiv e-prints*
- Stone, N., Sari, R., & Loeb, A. 2013, *MNRAS*, 435, 1809
- Tchekhovskoy, A., Metzger, B. D., Giannios, D., & Kelley, L. Z. 2014, *MNRAS*, 437, 2744
- van Velzen, S., Farrar, G. R., Gezari, S., Morrell, N., Zaritsky, D., Östman, L., Smith, M., Gelfand, J., & Drake, A. J. 2011, *ApJ*, 741, 73